A Nonenzymatic Hydrogen Peroxide Sensor Based on Pt/PPy Hollow Hybrid Microspheres

Yulin Li, Yunzhen Chang, Ming Jin, Yanyun Liu, Gaoyi Han

Institute of Molecular Science, Key Laboratory of Chemical Biology of Molecular Engineering of Education Ministry, Shanxi University, Taiyuan 030006, China

Received 28 February 2011; accepted 2 February 2012
DOI 10.1002/app.36939
Published online in Wiley Online Library (wileyonlinelibrary.com).

ABSTRACT: The surface of silica particles was NH_2— functionalized by 3-aminopropyltrimethoxysilane, then the platinum/polypyrrole hybrid hollow microspheres were prepared by treating the SiO_2 template decorated by the H_2PtCl_6 via the NH_2— group with pyrrole vapor and developed as hydrogen peroxide (H_2O_2) sensor. The platinum/polypyrrole hybrid hollow sphere materials were characterized by transmission electron microscopy and infrared spectroscopy, and the catalytic electrodes were investigated by electrochemical method. The results showed that the nonenzymatic sensor displayed a good electro-catalytic response and high sensitivity to the oxidation of H_2O_2, and the resulting sensor showed a wide linear range from 1.9 to 9.7 m*M* H_2O_2. The obvious response could be still observed in i–t curve when the concentration of H_2O_2 was as low as 1.0 μ*M*. © 2012 Wiley Periodicals, Inc. J Appl Polym Sci 000: 000–000, 2012

Key words: conducting polymers; polypyrrole; electrochemistry; Pt nanoparticles; hydrogen peroxide sensor

INTRODUCTION

The determination of H_2O_2 is of importance in industrial, clinical, and many other fields. Many H_2O_2 analytical methods including titrimetry, spectro-photometry, chemi-luminescence, and electrochemistry have been developed.[1–5] Among aforementioned analytical methods, the electrochemical technique has been widely used because of its fast response and low cost. Since the first sensor for hydrogen peroxide in 1967, the developments of novel sensor measuring H_2O_2 have aroused wide interest in the last years.[6] Many enzyme-based biosensors toward H_2O_2 oxidation have been fabricated,[7–10] but the application of these H_2O_2 enzymatic biosensors is limited partially due to disadvantage of their rigorous environment, high cost, instability of enzymes, and the complicated process of enzyme immobilization.[11–13] When compared with enzyme-base sensor, nonenzymatic sensors show high stability, which is free of influence of temperature.

Conducting polymers/metal hybrid materials exhibit many excellent properties because of the combination of the different properties of the each component. It has reported that conducting polymers are good supporting matrixes for nanoparticles (NPs).[14,15] Polypyrrole (PPy) as one of the most popular conducting polymers has attracted a great deal of interest for its potential application in batteries, supercapcacitors, microwave shielding, sensors, and actuators because of their highly electrical conductivity, good stability, and easy preparation.[16–21] On the other hand, catalytic behaviors of the transition metal NPs, especially noble metal NPs, have been extensively studied because of their high catalytic activity for many chemical reactions.[22,23] In particular, Pt NPs have been demonstrated to low the H_2O_2 oxidation-reduction overvoltage efficiently and been studied to the catalytic activity of H_2O_2 reduction.[14,24–28] Furthermore, Pt NPs also exhibits good eletrocatalytic activity toward the oxidation of methanol, reduction of oxygen, and oxidation of glucose.[29–32]

In this article, by combing the advantages of PPy and Pt NPs, a hydrogen peroxide sensor has been constructed. In the process of preparation, the NH_2-functionalized SiO_2 was used as a template to adsorb H_2PtCl_6 and provide a reaction place for H_2PtCl_6 and pyrrole vapor. After the PPy and Pt NPs formed on the surface of the SiO_2, the SiO_2 core

Correspondence to: G. Han (han_gaoyis@sxu.edu.cn).

Contract grant sponsor: National Natural Science Foundation of China; contract grant numbers: 21073115, 20604014.

Contract grant sponsor: Natural Science Foundation of Shanxi Province; contract grant number: 2007021008.

Contract grant sponsor: Program for New Century Excellent Talents in University of China; contract grant number: NCET-10-0926.

Contract grant sponsor: Program for the Top Young and Middle-Aged Innovative Talents of Higher Learning Institutions of Shanxi Province (TYMIT and TYAL).

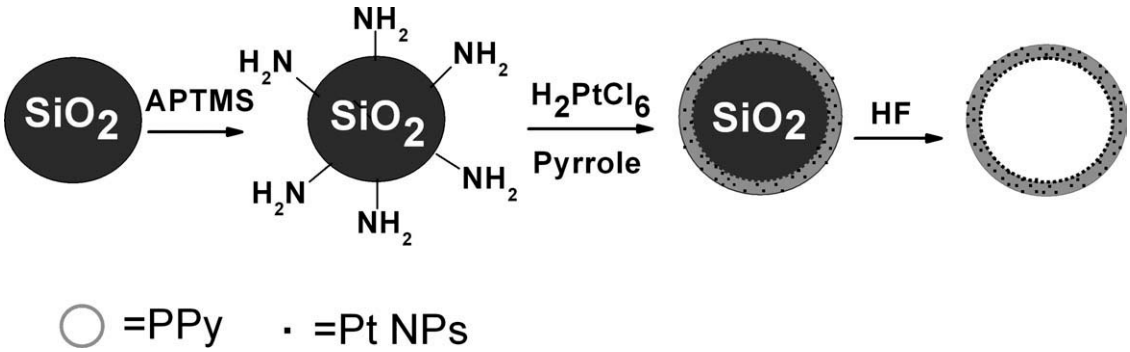

Scheme 1 The illustration of the formation of Pt/PPy hollow spheres.

was removed by HF, and then the hollow PPy microsphere on the inner surface decorated with Pt NPs formed. The electrodes modified with the Pt/PPy hybrid hollow microspheres were investigated and the results show that the hybrid material could be developed as new materials for no enzyme H_2O_2 sensor.

EXPERIMENTAL

Reagents

Pyrrole, dihydrogen hexachloroplatinate ($H_2PtCl_6 \cdot 6H_2O$), and 3-aminopropyltrimethoxy-silane (APTMS) were purchased from Guoyao Chemical Regent (Shanghai, China), and the pyrrole was distilled under reduced pressure before use. Tetraethyl orthosilicate (TEOS), hydrofluoric acid, and ammonium hydroxide were analytical grade and used as received. The aqueous solution of H_2O_2 was freshly prepared with 30% H_2O_2 just before use. All solutions were prepared using doubly distilled water.

Preparation of NH_2-fuctionalized silica nanoparticles

The NH_2-fuctionalized silica NPs were prepared according to the Stober method.[33] Briefly, 1.0 mL of TEOS was added into the 20.0 mL ethanol solution containing 1.2 mL ammonium hydroxide under vigorous stirring. After the mixture was allowed to stir at room temperature for 12 h, 150 μL of APTMS was added into the mixed solution. After the mixture was further stirred under room temperature for 12 h, 1.0 mL of NH_2-fuctionalized silica particles were washed successively with ethanol and water four times by suspension-centrifugation procedure, respectively. After the washed NH_2-modified SiO_2 particles were redispersed in 1.0 mL water, 75 μL of H_2PtCl_6 (the content of Pt is 7.53 μg/μL) were added to the dispersion, and then the mixture turned to light yellow. After briefly washing by suspension-centrifugation procedure, the finally obtained 0.5 mL suspension was kept in a refrigerator at 4°C.

Preparation of the Pt/PPy modified gold electrode

Before modification, the gold electrode was polished with alumina polishing powder on a chammy to a mirror. After the electrode was sonicated in distilled water, ethanol, and distilled water for 10 min to remove any adhesive substances on the electrode surface, respectively. Then, 3.5 μL of the prepared SiO_2 particles decorated with Pt precursor suspension was dropped onto the gold electrode surface and dried at room temperature, followed by coating with 0.2 μL of 5 wt % Nafion and dried. Then, the modified electrode was put into a small bottle containing little amount of pyrrole for 0.5 h, during which the Pt precursor reacted with pyrrole vapor and the PPy and Pt NPs formed. After being dried in air, this electrode was rinsed with methanol for 5.0 min and dried at ambient atmosphere. Then, the electrode was immersed in the hydrofluoric acid for 10.0 min. Finally, the modified electrode was washed gently by water several times and dried, then the Pt/PPy hollow sphere was successfully assembled on Au electrode. The procedure was shown in Scheme 1. The sample for TEM and IR measure was prepared at similar procedure without adding the Nafion solution.

Characterization and electrochemical measurement

The morphology of the hybrid SiO_2/Pt/PPy and the hybrid hollow sphere of Pt/PPy were observed by using a transmission electron microscope (JEM-1011). Infrared spectra were recorded on a Nicolet 380 Fourier transform infrared spectrometer (FTIR) with 4 cm^{-1} resolution (KBr pellets). Amperometric and Cyclic voltammetry (CV) experiments were performed on an electrochemical work station (Autolab, μ3Aut71035, The Netherland). All electrochemical experiments were carried out using a conventional three-electrode system, and a gold electrode with 2.0 mm diameter modified by the hybrid Pt/PPy hollow sphere, a thin platinum sheet, and a saturated calomel electrode were used as the work, auxiliary and reference electrode, respectively. All of electrochemical

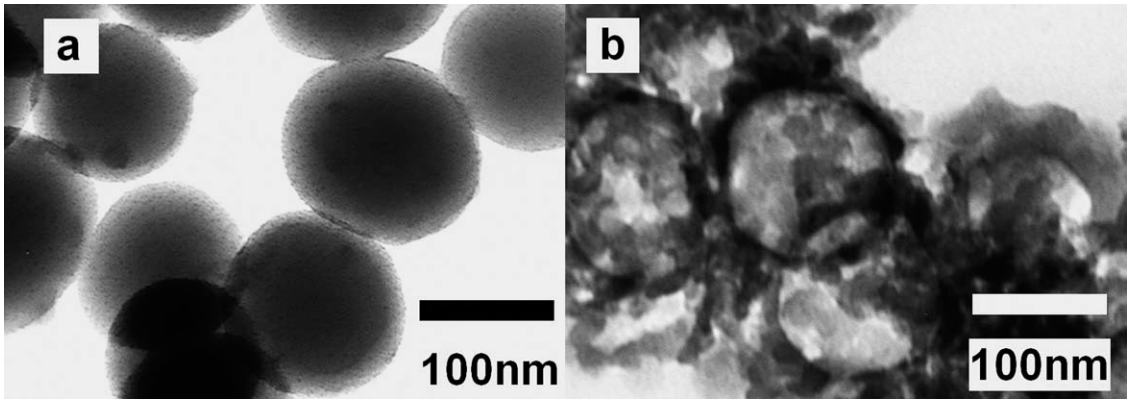

Figure 1 TEM images of (a) SiO_2/Pt/PPy composites and (b) Pt/PPy hybrid spheres.

experiments were carried out at room temperature in 30 mL of 0.1*M* phosphate buffer (pH = 7.2) containing 0.1*M* KCl.

RESULTS AND DISCUSSION

Characterization of the SiO_2/Pt/PPy and Pt/PPy hybrid materials

From the TEM image shown in Figure 1(A), we can find that the SiO_2/Pt/PPy hybrid particles with diameter about 140 nm exhibit apparent core-shell-like morphology, the diameter of the SiO_2 is about 100 nm and the thickness of the shell range from 8 to 20 nm. Furthermore, it can be seen that the high density of Pt NPs with the size of about 4 nm disperse on the spheres. After the SiO_2 cores are removed by hydrofluoric acid, the hollow Pt/PPy hybrid spheres [Fig. 1(B)] are obtained, we can clearly find that some holes exhibit on the hybrid spheres.

From the FTIR spectra of SiO_2/Pt/PPy and Pt/PPy shown in Figure 2, it can be found that hat the sample of SiO_2/Pt/PPy shows the characteristic vibration of PPy and SiO_2. In the sample of SiO_2/Pt/PPy, the peak at 1090 cm^{-1} can assigned to the stretching vibration of Si—O—Si, whereas the absorption peaks at 800 cm^{-1} and 462 cm^{-1} may be induced by the circular Si—O bond.[34] For Pt/PPy, the peak at 1715 cm^{-1} is due to the stretching of carbonyl group, indicating that the over-oxidation of PPy occurs during the process of chemical polymerization.[35,36] The peak at 1556 cm^{-1} peak is assigned to the C=C vibration of pyrrole rings while the bands at 1458, 1422, and 1362 cm^{-1} are due to C=N vibrations and C—H deformations, respectively.[36,37] The 1223 cm^{-1} band may be attributed to the breathing vibration of the pyrrole ring. The bands of C—H and N—H in-plane deformation vibration are located at 1036 cm^{-1}, whereas the band of C—H out-of-plane deformation vibration is found at 927 cm^{-1} and 740 cm^{-1}.[38,39]

Electrochemical performances of the Pt/PPy hollow spheres modified Au electrode toward hydrogen peroxide

To obtain the optimum activity of the electrodes, different amount of the SiO_2 decorated with Pt precursor is used to drop on the electrode surface and react with pyrrole vapor, we find that the modified electrodes exhibit the optimum activity when 3.5 μL of SiO_2 decorated with Pt precursor is used, so this amount is chosen in the subsequent experiments. From the CV curves shown in Figure 3(A), it can be seen that the bare Au electrode exhibits no obvious electrochemical response [Fig. 3(A)-a,d] whether in the PBS buffer solution or containing 1.0 m*M* H_2O_2 at the scan rate of 100 mV/s, whereas the electrodes modified with the SiO_2/Pt/PPy particles show some electro-oxidation activity and the peak current reach to 2.63 μA in the PBS buffer containing 1.0 m*M* H_2O_2. However, the electrodes modified with the hollow spheres of Pt/PPy hybrid material exhibit high electro-catalytic activity to H_2O_2 oxidation [Fig. 3(A)-d,f] and the current for H_2O_2 oxidation begin to increase at 0.23 V, then increase dramatically at 0.4 V until reach the maximum current of 11.2 μA at

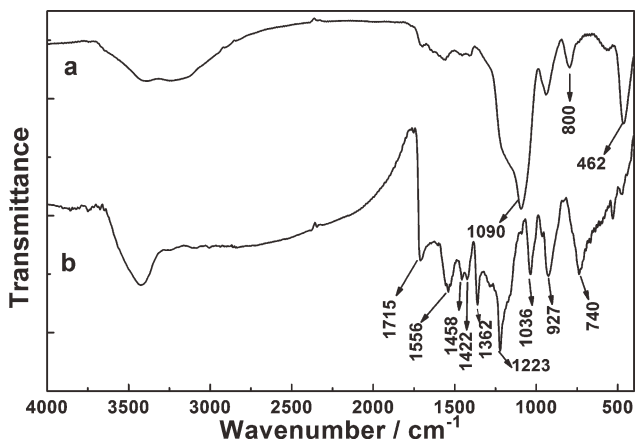

Figure 2 The FTIR spectra of (a) SiO_2/Pt/PPy composites and (b) Pt/PPy hybrid spheres.

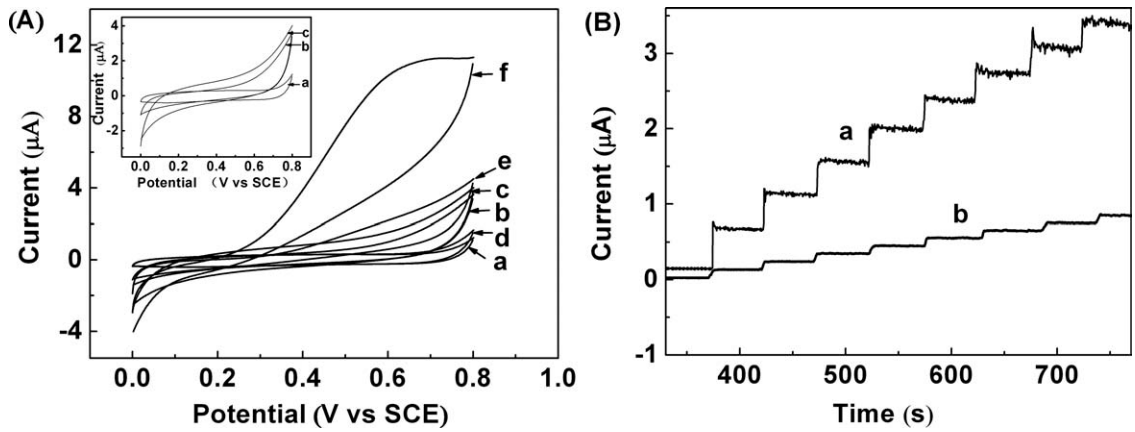

Figure 3 (A) the CV curves of bare Au electrode [(a) and (d)], the electrode modified by SiO_2/Pt/PPy [(b) and (e)] and Pt/PPy hollow microspheres modified electrode [(c) and (f)] in a 0.1*M* PBS buffer in the absence [(a–c)] or presence of 1.0 m*M* H_2O_2 [(d–f)]. (B) The amperometric response of the sensor fabricated by Pt/PPy hollow spheres (a) and Pt/PPy/SiO_2 (b) with successively injecting 0.1 m*M* H_2O_2 to the 0.1*M* PBS (pH = 7.2) during the test.

0.68 V. The curves of the amperometric response versus time are shown in Figure 3(B), from the curves, it can be seen that the current response dramatically increases on the electrode modified with hollow spheres of Pt/PPy with the increase of H_2O_2 concentration in the electrolyte solution continuously, whereas the current response increase slowly when the SiO_2/Pt/PPy particles are used as the modified material on the surface of the Au electrode. From above results, we can deduce that the Pt NPs are mainly dispersed on the inner surfaces of the hollow spheres, which is different from the most previous reports. When the SiO_2 particles exhibit as core, the Pt NPs are between the SiO_2 surface and the PPy shell, which prevent the H_2O_2 from Pt catalyst, when the SiO_2 cores are removed, the most Pt NPs emerge to the H_2O_2, which cause the current increase dramatically.

To get more information about the electrodes modified with hollow spheres of Pt/PPy, the current response of the electrodes at different scan rate are recorded in 0.1*M* PBS containing 1.0 m*M* H_2O_2 and the results are shown in Figure 4(A), it is found that the peak current increases linearly with the square root of the scan rate in the range of 20–140 mV/s, which indicate that the hollow spheres of Pt/PPy hybrid adhere to the electrode surface closely, and the catalytic reaction is diffusion-controlling at this scan rate range. Therefore, it can be concluded that the Pt/PPy hybrid materials can facilitate electron transfer between Pt NPs and electrode. The reaction may be occur as following: H_2O_2 molecules diffused and are adsorbed on the surface of Pt NPs, and followed by releasing two electrons, subsequently, during the process PPy help the electron transfer from Pt NPs to electrode.[14] The curves of CV of the electrodes modified with hollow spheres of Pt/PPy in 0.1*M* PBS buffer containing different concentration of H_2O_2 are shown in Figure 4(B). The oxidation

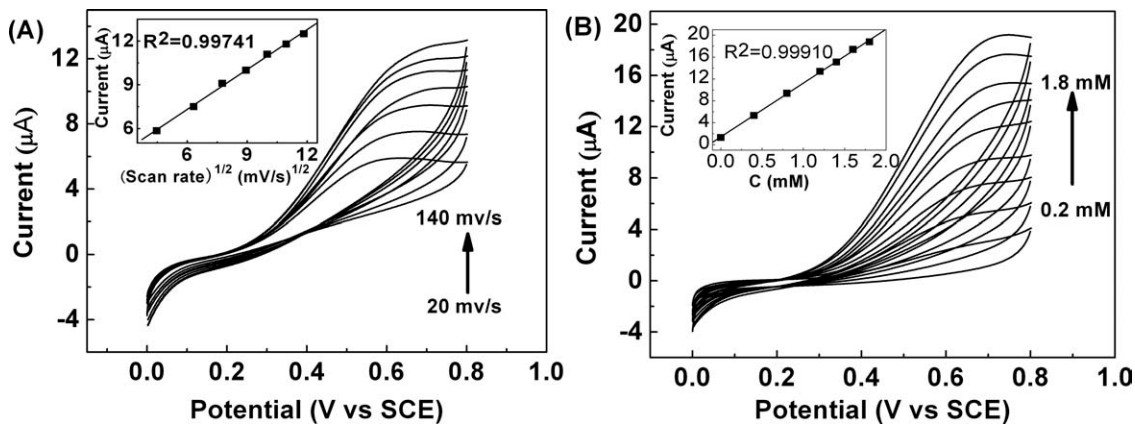

Figure 4 (A) CVs of modified Au electrode in 0.1*M* PBS (pH = 7.2) in the presence of 1.0 m*M* H_2O_2 with different scan rates (from the bottom: 20, 40, 60, 80, 100, 120, 140 mV/s). The inset shows the calibration plot of oxidation peak current versus the square root scan rate.(B) CVs of modified Au electrode in 0.1*M* PBS in the presence of H_2O_2 with different concentrations (from the bottom: 0.2, 0.4, 0.6, 0.8, 1.0, 1.2, 1.4, 1.6, 1.8 m*M*). Scan rate:100 mV/s. The inset shows the calibration plot of oxidation peak current versus H_2O_2 concentration.

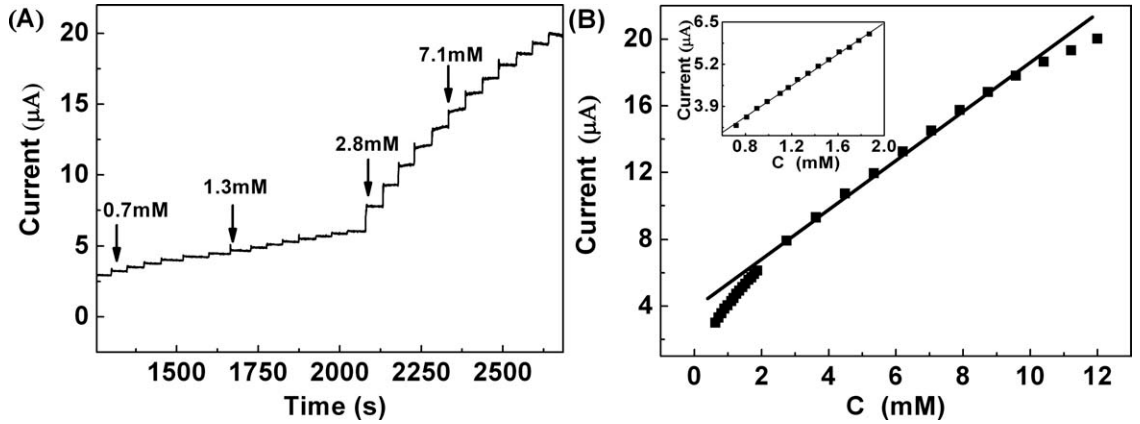

Figure 5 (A) Amperometric i–t curves of the sensor at the constant potential of 0.7 V in 0.1*M* PBS (pH = 7.2) with successive injection of H_2O_2. A potential of 0.7 V (vs. SCE) was applied on the working electrode during the measurement. (B) The calibration plot of oxidation current of H_2O_2 versus its concentration. The inset shows calibration plot in the low concentration of H_2O_2 concentration (from 0.7 to 1.9 m*M*).

peak current increases gradually from 3.08 to 18.8 μA when the concentration of H_2O_2 increases from 0.2 to 1.8 m*M*. The plot of the peak current response versus the concentration of the H_2O_2 illustrates that the addition of H_2O_2 to the supporting electrolyte resulted in a nearly linear increase in peak current for the oxidation of H_2O_2 ($R^2 = 0.99910$).

Figure 5(A) shows amperometric i–t curves of the sensor at the constant potential of 0.7 V in 0.1*M* PBS (pH = 7.2) with successive injection of H_2O_2 in the range of 0.7–12 m*M*. From Figure 5(B), it can be seen a good linear relationship between the catalytic current and H_2O_2 concentration from 1.9 to 9.6 m*M* (correlation coefficient: $R^2 = 0.99657$, $n = 10$). Furthermore, in the low concentration [the inset of Fig. 5(B)], the plot of the current versus H_2O_2 concentration exhibits a relatively high slope, the linear regression equation can be expressed as I (μA) = 1.56304 + 2.47592 C_{H_2O2} (m*M*). Although the concentration of H_2O_2 is in the range of 1.9–9.6 m*M*, the regression equation can be expressed as I (μA) = 3.31857 + 1.4311 C_{H_2O2} (m*M*), the slope is relatively small. This phenomenon is similar to the other literature.[40]

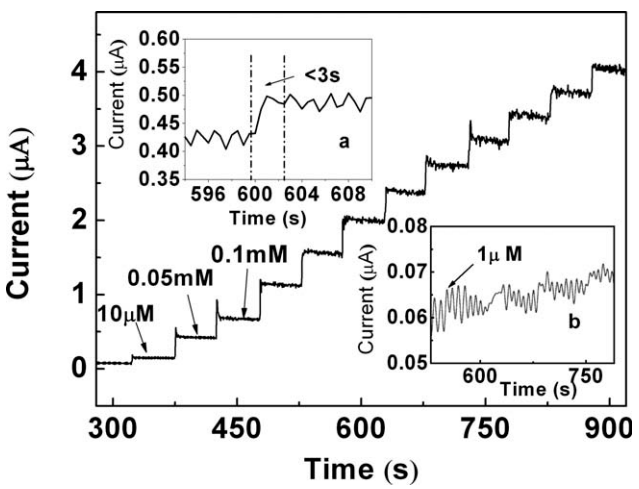

Figure 6 Amperometric i–t curves of the sensor electrode at the constant potential of 0.7 V in 0.1*M* PBS (pH = 7.2) with successive injection of H_2O_2. The inset (a) shows the amperometric response curves from 592 s to 610 s. The inset (b) shows the amperometric i–t curves with successive injection of 1.0 μ*M* H_2O_2.

The plot of the amperometric response versus time is shown in Figure 6, when the H_2O_2 solution is injected into the PBS buffer at an applied potential of 0.7 V, the current response on the modified electrode increases rapidly to a steady-state current value. It can be found that the sensors exhibit a quick response, for example, the current can increase to the maximum steady-state within 3.0 s after more H_2O_2 is added into the solution [the inset (a)]. The fast response should be attributed to the structure of Pt nanoparticles attached on the PPy inner microspheres closely, and then the hollow sphere adhere to the electrode surface closely, which make the electron transfer from H_2O_2 to electrode easily. Besides, the detection limit of this kind sensor is carefully measured and it is found that the obvious current response can still be observed when the concentration of the H_2O_2 is as low as 1.0 μ*M* [the inset (b)], which is lower than certain enzyme-based biosensor[7,9,41,42] and similar to the result reported in the literature.[14] These results show that the Pt/PPy hollow hybrid microspheres have good electrocatalytic activity toward H_2O_2 and may be used to fabricate the sensor for H_2O_2 with high response and high sensitivity.

CONCLUSIONS

In summary, we have fabricated a novel electrochemical sensor with Pt/PPy hybrid hollow microspheres by using NH_2-functionized SiO_2 as template. Comparing with Pt/PPy/SiO_2 microspheres, Pt/PPy

hollow structure modified Au electrode exhibits excellently electrocatalytic activity toward the oxidation of H_2O_2. In addition, the modified electrode shows a fast response (<3.0 s) and a detection limit of 1.0 μM.

References

1. Ma, L. P.; Yuan, R.; Chai, Y. Q.; Chen, S. H. J Mol Catal B 2009, 56, 215.
2. Wang, H. S.; Pan, Q. X.; Wang, G. X. Sensors 2005, 5, 266.
3. Chen, S. H; Yuan, R.; Chai, Y. Q.; Yin, B.; Li, W.; Min, L. Electrochim Acta 2009, 54, 3039.
4. Zhang, H. S.; Lai, G. H.; Han, D. Y.; Yu, A. M. Anal Bioanal Chem 2008, 390, 971.
5. Thenmozhi, K.; Narayanan, S. S. Anal Bioanal Chem 2007, 387, 1075.
6. Lupu, A.; Lisboa, P.; Valsesia, A. Sens Actuators B 2009, 137, 56.
7. Zhou, K. F.; Zhu, Y. H.; Yang, X. L.; Luo, J. Electrochim Acta 2010, 55, 3055.
8. Vianello, F.; Zennaro, L.; Rigo, A. Biosens Bioelectron 2007, 22, 2694.
9. Kafi, A. K. M.; Wu, G. S.; Chen, A. C. Biosens Bioelectron 2008, 24, 566.
10. MalaEkangyke, E. M. I.; Preethichandra, D. M. G.; Kaneto, K. Sens Actuators B 2008, 132, 166.
11. Zhou, C. Z.; Ju, H. X. Anal Chem 2004, 76, 6871.
12. Jia, J. B.; Wang, B. Q.; Wu, A. G.; Cheng, G. J.; Li, Z.; Dong, S. J Anal Chem 2002, 74, 2217.
13. Lin, J. H.; Zhang, L. J.; Zhang, S. S. Anal Biochem 2007, 320, 180.
14. Bian, X. J.; Lu, X. F.; Jin, E.; Kong, L. R.; Zhang, W. J.; Wang, C. Talanta 2010, 81, 813.
15. Roy, A. S.; Anilkumar, K. R.; Prasad, M. V. N. A. J Appl Polym Sci 2011, 121, 675.
16. Feng, C. Q.; Chew, S. Y.; Guo, Z. P.; Liu, H. K. J Power Sources 2007, 174, 1095.
17. Fan, L. Z.; Hu, Y. S.; Maier, J.; Adelhelm, P.; Smarsly, B.; Antroietti, M. Adv Funct Mater 2007, 17, 3083.
18. Hakansson, E.; Amiet, A.; Kaynaka, K. A. Synth Met 2006, 156, 17.
19. Han, G. Y.; Shi, G. Q. Thin Solid Films 2007, 515, 6986.
20. Han, G. Y.; Shi, G. Q. J Electroanal Chem 2004, 569, 169.
21. Han, G. Y.; Shi, G. Q. Sens Actuators B 2004, 99, 525.
22. Zen, J. M.; Kumar, A. S.; Chang, C. R. Anal Chem 2003, 75, 2703.
23. Hrapovic, S.; Luong, J. H. T. Anal Chem 2003, 75, 3308.
24. Chi, Q.; Dong, A. Anal Chim Acta 1993, 279, 17.
25. Ikariyama, Y.; Yamanechi, S. J Electrochem Soc 1989, 136, 702.
26. Miscoria, S. A.; Barrera, G. D.; Rivas, G. A. Electroanalysis 2002, 14, 981.
27. Sakslund, H.; Wang, J. J Electronal Chem 1994, 374, 71.
28. Shankaran, D. R.; Uehara, N.; Kato, T. Biosens Bioeletron 2003, 18, 721.
29. Zhou, W. Q.; Du, Y. K.; Ren, F. F.; Wang, C. Y.; Xu, T. K. Int J Hydrogen Energy 2010, 35, 3270.
30. Liu, X. M.; Li, M. Y.; Han, G. Y.; Dong, J. H. Electrochim Acta 2010, 55, 2983.
31. Malheiro, A. R.; Perez, J.; Villullas, H. M. J Power Sources 2010, 195, 7255.
32. Chun, X.; Duan, D. X.; Shen, G. L.; Yu, R. Q. Talanta 2007, 71, 2040.
33. Stöber, W.; Fink, A. J Colloid Interface Sci 1968, 26, 62.
34. Ryu, S. R.; Tomozawa, M. J Non-Cryst Solids 2006, 352, 3929.
35. Mathys, G. I.; Truong, V. T. Synth Met 1997, 89, 103.
36. Han, G. Y.; Shi, G. Q.; Yuan, J. Y.; Chen, F. E. J Mater Sci 2004, 39, 4451.
37. Han, G. Y.; Shi, G. Q.; Qu, L. T.; Yuan, J. Y.; Chen, F. E.; Wu, P. Y. Polym Int 2004, 53, 1554.
38. Vishnuvardhan, T. K.; Kulkarni, V. R.; Basavaraja, C.; Raghavendra, S. C. Bull Mater Sci 2006, 29, 77.
39. Amparat, R. U. R.; Artita, P. J.; Walaiporn, P. O.; Sirisart, O. J Met Mater Miner 2008, 18, 27.
40. Miao, X. X.; Yuan, R.; Chai, Y. Q.; Shi, Y. T.; Yuan, Y. Y. J Electroanal Chem 2005, 577, 273.
41. Wang, L.; Wang, E. K. Electrochem Commun 2004, 6, 225.
42. Lei, C. X.; Hu, S. Q.; Shen, G. L.; Yu, R. Q. Talanta 2003, 59, 981.